

Appendix to:
“The evolution of stage-specific virulence: differential selection
of parasites in juveniles ” to be published at *Evolution Letters*;
doi: 10.1002/evl3.105

Ryosuke Iritani, Elisa Visher & Mike Boots

February 18, 2019

Contents

A	Invasion analysis	2
A.1	Generalized ODE	2
A.2	Stage-period	2
A.3	Mutant dynamics	3
A.4	Invasion fitness and invadability condition	5
A.5	Selection gradient for adult virulence	7
A.6	Reproductive values	7
A.7	Selection gradient for juvenile virulence	9
A.8	Graph-theoretical approach	10
A.9	Attainability and Evolutionary stability	11
A.10	Condition for parasite persistence	15
A.11	When $\rho = 1$ (fully assortative transmission)	16
B	Robustness	16
B.1	Recovery	17
B.2	Susceptibility	17
B.3	Tolerance	17
B.4	Infectiousness	18
B.5	Density-dependent transmission	18
B.6	Fecundity virulence and evolutionarily stable resource shifts	18
C	Generalized pathway structure	18

1 A Invasion analysis

2 A.1 Generalized ODE

3 The epidemiological dynamics is given by:

$$\begin{aligned}
 \frac{dS_J}{dt} &= (r - \kappa(S_A + I_A)) \cdot (S_A + I_A) - (u + \phi_{JA} + \phi_{JJ} + m_J) S_J + \gamma_J I_J, \\
 \frac{dS_A}{dt} &= u S_J - (m_A + \phi_{AJ} + \phi_{AA}) S_A + \gamma_A I_A, \\
 \frac{dI_J}{dt} &= (\phi_{JA} + \phi_{JJ}) S_J - (u + m_J + v_J + \gamma_J) I_J, \\
 \frac{dI_A}{dt} &= (\phi_{AJ} + \phi_{AA}) S_A + u I_J - (m_A + v_A + \gamma_A) I_A,
 \end{aligned}
 \tag{A.1}$$

4 with the notation explained in the main text; here, for the sake of generality, we incorporated recovery γ_J, γ_A , which
 5 we will use later. Solving the system gives two equilibria: one is disease free $(S_J^{(0)}, S_A^{(0)}, 0, 0)$, and the other is
 6 endemic $(S_J^\#, S_A^\#, I_J^\#, I_A^\#)$.

7 A.2 Stage-period

8 In this subsection, we will restrict our attention to the disease-free subsystem:

$$\begin{aligned}
 \frac{dS_J}{dt} &= (r - \kappa S_A) S_A - (u + m_J) S_J, \\
 \frac{dS_A}{dt} &= u S_J - m_A S_A.
 \end{aligned}
 \tag{A.2}$$

9 First, the probability of successful maturation is given by:

$$\pi_S = \frac{u}{u + m_J}.
 \tag{A.3}$$

10 Second, consider two random variables: the duration of time a host individual spends as a juvenile, denoted T_J , and
 11 the duration of time a host individual spends as an adult, denoted T_A . The fate of a juvenile is (i) to die as a juvenile
 12 or (ii) to successfully mature and die as an adult. For the former case, which occurs with probability $1 - \pi_S$, the
 13 random variable T_J follows an exponential distribution with mean $1/(u + m_J)$ while $T_A \equiv 0$. With probability π_S ,
 14 the latter happens, in which case, the bivariate random variables (T_J, T_A) follow the two dimensional exponential
 15 distribution, given by:

$$(T_J, T_A) \text{ follows } (u + m_J) e^{-(u+m_J)T_J} \cdot m_A e^{-m_A T_A}.
 \tag{A.4}$$

16 Therefore, the expectation of $T_A/(T_J + T_A)$ is given by:

$$\theta_A = (1 - \pi_S) \cdot 0 + \pi_S \cdot \iint_0^\infty \frac{T_A}{T_J + T_A} (u + m_J) e^{-(u+m_J)T_J} \cdot m_A e^{-m_A T_A} dT_J dT_A. \quad (\text{A.5})$$

17 To calculate the integral, we carry out the variable transformation by:

$$L := T_J + T_A, f_A := \frac{T_A}{T_J + T_A} \iff T_J = L(1 - f_A), T_A = Lf_A, \quad (\text{A.6})$$

18 with the corresponding Jacobian of the variable transformation:

$$\frac{\partial(T_J, T_A)}{\partial(L, f_A)} := \left| \det \begin{pmatrix} \frac{\partial T_J}{\partial L} & \frac{\partial T_J}{\partial f_A} \\ \frac{\partial T_A}{\partial L} & \frac{\partial T_A}{\partial f_A} \end{pmatrix} \right| = L (> 0). \quad (\text{A.7})$$

19 Noting that $0 \leq f_A \leq 1$, we have:

$$\begin{aligned} \theta_A &= \frac{u}{u + m_J} \iint_0^\infty \frac{T_A}{T_J + T_A} (u + m_J) e^{-(u+m_J)T_J} \cdot m_A e^{-m_A T_A} dT_J dT_A \\ &= \frac{u}{u + m_J} \int_0^1 \int_0^\infty f_A \cdot (u + m_J) \cdot m_A \cdot e^{-((u+m_J)(1-f_A)+m_A f_A)L} L dL df_A. \end{aligned} \quad (\text{A.8})$$

20 Integrating with respect to L firstly and then integrating with respect to f_A , we have:

$$\theta_A = \frac{u}{u + m_J - m_A} \left(1 + \frac{m_A}{u + m_J - m_A} \cdot \log \left(\frac{m_A}{u + m_J} \right) \right), \quad (\text{A.9})$$

21 as shown in the main text.

22 Note that if $u + m_J = m_A$, then θ_A is of the form “0/0”. As such θ_A is interpreted as the limit $\lim_{m_A \rightarrow u+m_J} = \pi_S/2$,
 23 which is the probability of maturation (π_S) times the conditional expectation of the fraction of sub-lifespan as an
 24 adult (given that a sampled adult host has matured into an adult). This calculation is obtained by setting $\exp(\varepsilon) :=$
 25 $m_A/(u + m_J)$ and using the Taylor expansion $\exp(\varepsilon) = 1 + \varepsilon + \frac{\varepsilon^2}{2} + \mathcal{O}(\varepsilon^3)$ where $\mathcal{O}()$ represents the Landau’s big- \mathcal{O}
 26 for $\varepsilon \rightarrow +0$. Exact computation including the evaluation of integral is shown in a Mathematica-code (SI Fig 1).

27 A.3 Mutant dynamics

28 Hereafter, without special remarks, we will assume that $\rho \lesssim 1$ (i.e., transmission can occur between classes).

29 When $\rho = 1$, as shown in Osnas & Dobson (2011), a special treatment is needed.

Evaluating the stage-period requires variable-transformation,
but Mathematica can skip this task.

```
In[12]:= Assuming[mA > 0 && mJ > 0 && u > 0, u / (u + mJ) *  
Integrate[tA / (tA + tJ) * (u + mJ) * mA *  
Exp[-(u + mJ) * tJ] * Exp[-(mA) * tA],  
{tJ, 0, +∞}, {tA, 0, +∞}]]];  
Out[12]= % - u / (u + mJ - mA) *  
(1 + mA / (u + mJ - mA) * Log[mA / (u + mJ)]) //  
Simplify  
Out[12]= 0  
...as desired.  
In[13]:= Limit[%, mA → +u + mJ]  
Out[13]=  $\frac{u}{2(mJ + u)}$   
...as desired.
```

SI Figure 1: Mathematica code for evaluating the stage-period.

30 The dynamics governing the mutant's growth rate (mutant dynamics) reads:

$$\begin{aligned}
\frac{dI'_J}{dt} &= (\phi'_{JA} + \phi'_{JJ}) S_J^\# - (u + m_J + v'_J + \gamma_J) I'_J \\
&= (\phi'_{JA} + \phi'_{JJ}) S_J^\# - \mu'_J I'_J, \\
\frac{dI'_A}{dt} &= (\phi'_{AJ} + \phi'_{AA}) S_A^\# + u I'_J - (m_A + v'_A + \gamma_A) I'_A \\
&= (\phi'_{AJ} + \phi'_{AA}) S_A^\# + u I'_J - \mu'_A I'_A.
\end{aligned} \tag{A.10}$$

31 Here,

$$\begin{aligned}
\phi'_{JJ} &= \frac{\alpha_J \sigma_{JJ} \beta'_J I'_J}{S_J^\# + S_A^\# + I_J^\# + I_A^\#}, \\
\phi'_{JA} &= \frac{\alpha_J \sigma_{JA} \beta'_A I'_A}{S_J^\# + S_A^\# + I_J^\# + I_A^\#}, \\
\phi'_{AJ} &= \frac{\alpha_A \sigma_{AJ} \beta'_J I'_J}{S_J^\# + S_A^\# + I_J^\# + I_A^\#}, \\
\phi'_{AA} &= \frac{\alpha_A \sigma_{AA} \beta'_A I'_A}{S_J^\# + S_A^\# + I_J^\# + I_A^\#}.
\end{aligned} \tag{A.11}$$

32 A.4 Invasion fitness and invadability condition

33 Linearizing the mutant dynamics around the endemic equilibrium, we get a corresponding Jacobian:

$$\begin{aligned}
\mathbf{J}' &= \begin{pmatrix} \frac{\alpha_J S_J^\# \sigma_{JJ} \beta'_J}{S_J^\# + S_A^\# + I_J^\# + I_A^\#} & \frac{\alpha_J S_J^\# \sigma_{JA} \beta'_A}{S_J^\# + S_A^\# + I_J^\# + I_A^\#} \\ \frac{\alpha_A S_A^\# \sigma_{AJ} \beta'_J}{S_J^\# + S_A^\# + I_J^\# + I_A^\#} & \frac{\alpha_A S_A^\# \sigma_{AA} \beta'_A}{S_J^\# + S_A^\# + I_J^\# + I_A^\#} \end{pmatrix} - \begin{pmatrix} \mu'_J & 0 \\ -u & \mu'_A \end{pmatrix} \\
&= \mathbf{B}' - \mathbf{D}'.
\end{aligned} \tag{A.12}$$

34 The next generation matrix \mathbf{G}' is given by:

$$\begin{aligned}
\mathbf{G}' &= \mathbf{B}' (\mathbf{D}')^{-1} \\
&= \begin{pmatrix} a'_{JJ} & a'_{JA} \\ a'_{AJ} & a'_{AA} \end{pmatrix} \\
&= \begin{pmatrix} \frac{\alpha_J S_J^\# \sigma_{JJ} \beta'_J}{S_J^\# + S_A^\# + I_J^\# + I_A^\#} & \frac{\alpha_J S_J^\# \sigma_{JA} \beta'_A}{S_J^\# + S_A^\# + I_J^\# + I_A^\#} \\ \frac{\alpha_A S_A^\# \sigma_{AJ} \beta'_J}{S_J^\# + S_A^\# + I_J^\# + I_A^\#} & \frac{\alpha_A S_A^\# \sigma_{AA} \beta'_A}{S_J^\# + S_A^\# + I_J^\# + I_A^\#} \end{pmatrix} \begin{pmatrix} \frac{1}{\mu'_J} & 0 \\ u & \frac{1}{\mu'_A} \end{pmatrix} \\
&= \begin{pmatrix} \frac{\alpha_J S_J^\# \sigma_{JJ} \beta'_J}{S_J^\# + S_A^\# + I_J^\# + I_A^\#} \cdot \frac{1}{\mu'_J} + \frac{\alpha_J S_J^\# \sigma_{JA} \beta'_A}{S_J^\# + S_A^\# + I_J^\# + I_A^\#} \cdot \frac{u}{\mu'_J \mu'_A} & \frac{\alpha_J S_J^\# \sigma_{JA} \beta'_A}{S_J^\# + S_A^\# + I_J^\# + I_A^\#} \cdot \frac{1}{\mu'_A} \\ \frac{\alpha_A S_A^\# \sigma_{AJ} \beta'_J}{S_J^\# + S_A^\# + I_J^\# + I_A^\#} \cdot \frac{1}{\mu'_J} + \frac{\alpha_A S_A^\# \sigma_{AA} \beta'_A}{S_J^\# + S_A^\# + I_J^\# + I_A^\#} \cdot \frac{u}{\mu'_J \mu'_A} & \frac{\alpha_A S_A^\# \sigma_{AA} \beta'_A}{S_J^\# + S_A^\# + I_J^\# + I_A^\#} \cdot \frac{1}{\mu'_A} \end{pmatrix}.
\end{aligned} \tag{A.13}$$

35 Elementary algebra of matrices gives the matrix-product form of \mathbf{G}' in the main text.

36 The dominant eigenvalue of \mathbf{G}' (denoted $\Lambda[\mathbf{G}']$) is given by:

$$\Lambda[\mathbf{G}'] = \frac{a'_{JJ} + a'_{AA} + \sqrt{(a'_{JJ} + a'_{AA})^2 - 4(a'_{JJ} a'_{AA} - a'_{JA} a'_{AJ})}}{2}. \tag{A.14}$$

37 Here note that under weak selection (i.e., when $|\mathbf{v}' - \mathbf{v}|$ is negligibly small) and the continuity of a'_{JJ} and a'_{AA} with
38 respect to \mathbf{v}' , we can show that:

$$a'_{JJ} + a'_{AA} < 2 \tag{A.15}$$

39 (see Appendix A.6; this inequality assures that the axis of symmetry of the characteristic function of \mathbf{G}' , which is a
40 quadratic function, lies on the left of 1). With Eqn (A.14), we can consequently say that $\Lambda[\mathbf{G}'] > 1$ (the invadability
41 condition) holds¹ if and only if:

$$w(\mathbf{v}', \mathbf{v}) := a'_{JJ} + a'_{AA} - (a'_{JJ} a'_{AA} - a'_{JA} a'_{AJ}) > 1. \tag{A.16}$$

42 Plugging Eqn (A.13) into Eqn (A.16) supplies:

$$w(\mathbf{v}', \mathbf{v}) = \alpha_J \frac{S_J^\#}{H^\#} \sigma_{JJ} \frac{\beta'_J}{\mu'_J} + \frac{u}{\mu'_J} \cdot \alpha_J \frac{S_J^\#}{H^\#} \sigma_{JA} \frac{\beta'_A}{\mu'_A} + \alpha_A \frac{S_A^\#}{H^\#} \sigma_{AA} \frac{\beta'_A}{\mu'_A} - (\sigma_{JJ} \sigma_{AA} - \sigma_{JA} \sigma_{AJ}) \frac{\alpha_J S_J^\# \alpha_A S_A^\#}{(H^\#)^2} \cdot \frac{\beta'_J \beta'_A}{\mu'_J \mu'_A}. \tag{A.17}$$

43 Using the shorthand notation for $\pi'_1 = u/\mu'_J$ (probability of successful maturation of juveniles infected by the mutant
44 strain), $R'_X = \beta'_X/\mu'_X$ (the production from a X-stage host during its infectivity duration), $q_{XY}^\# := \alpha_X S_X^\# \sigma_{XY}/H^\#$

¹The trick here is to isolate the square root on the left hand side and then square both sides.

45 (the availability of stage-X hosts from the perspective of the parasite infecting a stage-Y hosts), and $\rho = \sigma_{JJ}\sigma_{AA} -$
 46 $\sigma_{JA}\sigma_{AJ}$ (assortativity), with all these substituted, one can recover the invasion fitness measure given in the main
 47 text (Eq 6).

48 An elementary calculation (using the endemic condition for the ODE, $(S_J^\#, S_A^\#, I_J^\#, I_A^\#)$) yields $w(\mathbf{v}, \mathbf{v}) \equiv 1$ for
 49 any \mathbf{v} ; that is, the invasion fitness of a phenotypically neutral mutant is unity (and thus selectively neutral).

50 A.5 Selection gradient for adult virulence

51 Henceforth, by f° , we mean that we evaluate a quantity f at neutrality, $\mathbf{v}' = \mathbf{v}$. Partial differentiation of w with
 52 respect to v'_J, v'_A gives the selection gradient for the corresponding trait:

$$g_J(\mathbf{v}) = \left(\frac{\partial w(\mathbf{v}', \mathbf{v})}{\partial v'_J} \right) \Big|_{\mathbf{v}'=\mathbf{v}}, \quad (\text{A.18})$$

$$g_A(\mathbf{v}) = \left(\frac{\partial w(\mathbf{v}', \mathbf{v})}{\partial v'_A} \right) \Big|_{\mathbf{v}'=\mathbf{v}}. \quad (\text{A.19})$$

53 Upon some algebra, we get:

$$g_A(\mathbf{v}) = \left\{ \frac{\alpha_A S_A^\# \sigma_{AA}}{H^\#} \cdot \left(1 - \frac{\alpha_J S_J^\# \sigma_{JJ}}{H^\#} \cdot \frac{\beta_J}{\mu_J} \right) + \frac{\alpha_J S_J^\# \sigma_{JA}}{H^\#} \cdot \left(\frac{u}{\mu_J} + \frac{\alpha_A S_A^\# \sigma_{AJ}}{H^\#} \cdot \frac{\beta_J}{\mu_J} \right) \right\}^\circ$$

$$\times \left(\frac{\beta_A}{\mu_A} \right)^\circ \cdot \left(\frac{1}{\beta_A} \cdot \frac{d\beta_A}{dv_A} - \frac{1}{\mu_A} \right)^\circ. \quad (\text{A.20})$$

54 It is only the final factor that can change its sign (see Footnote 2 in Appendix A.7). To obtain the selection gradient
 55 for juvenile virulence, more tedious work is needed. As such, we will use Fisher's reproductive value (Fisher 1958;
 56 Taylor 1990; Frank 1998; Caswell 2001).

57 A.6 Reproductive values

58 We here provide the reproductive value-based approach. Note that the case $\rho = 1$ violates this approach.

We shall first remember:

$$\begin{aligned}
q_{JJ}^{\#} &= \frac{\alpha_J S_J^{\#} \sigma_{JJ}}{H^{\#}}, \\
q_{JA}^{\#} &= \frac{\alpha_J S_J^{\#} \sigma_{JA}}{H^{\#}}, \\
q_{AJ}^{\#} &= \frac{\alpha_A S_A^{\#} \sigma_{AJ}}{H^{\#}}, \\
q_{AA}^{\#} &= \frac{\alpha_A S_A^{\#} \sigma_{AA}}{H^{\#}}, \\
\pi_1' &= \frac{u}{\mu_J}, \\
R_J' &= \frac{\beta_J'}{\mu_J}, \\
R_A' &= \frac{\beta_A'}{\mu_A'};
\end{aligned} \tag{A.21}$$

then, we can get:

$$\begin{aligned}
\mathbf{G}' &= \begin{pmatrix} a'_{JJ} & a'_{JA} \\ a'_{AJ} & a'_{AA} \end{pmatrix} \\
&= \begin{pmatrix} \frac{\alpha_J S_J^{\#} \sigma_{JJ} \beta_J'}{H^{\#}} \cdot \frac{1}{\mu_J'} + \frac{\alpha_J S_J^{\#} \sigma_{JA} \beta_A'}{H^{\#}} \cdot \frac{u}{\mu_J' \mu_A'} & \frac{\alpha_J S_J^{\#} \sigma_{JA} \beta_A'}{H^{\#}} \cdot \frac{1}{\mu_A'} \\ \frac{\alpha_A S_A^{\#} \sigma_{AJ} \beta_J'}{H^{\#}} \cdot \frac{1}{\mu_J'} + \frac{\alpha_A S_A^{\#} \sigma_{AA} \beta_A'}{H^{\#}} \cdot \frac{u}{\mu_J' \mu_A'} & \frac{\alpha_A S_A^{\#} \sigma_{AA} \beta_A'}{H^{\#}} \cdot \frac{1}{\mu_A'} \end{pmatrix} \\
&= \begin{pmatrix} q_{JJ}^{\#} R_J' + \pi_1' q_{JA}^{\#} R_A' & q_{JA}^{\#} R_J' \\ q_{AJ}^{\#} R_J' + \pi_1' q_{AA}^{\#} R_A' & q_{AA}^{\#} R_A' \end{pmatrix}.
\end{aligned} \tag{A.22}$$

At neutrality,

$$\mathbf{G}^{\circ} = \begin{pmatrix} q_{JJ}^{\#} R_J^{\circ} + \pi_1 q_{JA}^{\#} R_A^{\circ} & q_{JA}^{\#} R_A^{\circ} \\ q_{AJ}^{\#} R_J^{\circ} + \pi_1 q_{AA}^{\#} R_A^{\circ} & q_{AA}^{\#} R_A^{\circ} \end{pmatrix}. \tag{A.23}$$

Since the eigenvalue of \mathbf{G}° is unity, premultiplying the left eigenvector $(\ell_J^{\circ}, \ell_A^{\circ})$ must return $(\ell_J^{\circ}, \ell_A^{\circ})$:

$$(\ell_J^{\circ}, \ell_A^{\circ}) \begin{pmatrix} q_{JJ}^{\#} R_J^{\circ} + \pi_1 q_{JA}^{\#} R_A^{\circ} & q_{JA}^{\#} R_A^{\circ} \\ q_{AJ}^{\#} R_J^{\circ} + \pi_1 q_{AA}^{\#} R_A^{\circ} & q_{AA}^{\#} R_A^{\circ} \end{pmatrix} = (\ell_J^{\circ}, \ell_A^{\circ}). \tag{A.24}$$

Although it is possible to analytically solve $(\ell_J^{\circ}, \ell_A^{\circ})$, it does not lead to a transparent expression. Therefore, we

64 instead derive the following (equivalent) relation:

$$\begin{pmatrix} \ell_J^\circ & \ell_A^\circ \end{pmatrix} (\mathbf{G}^\circ - \mathbf{I}) = \begin{pmatrix} \ell_J^\circ & \ell_A^\circ \end{pmatrix} \begin{pmatrix} q_{JJ}^\# R_J^\circ + \pi_1^\circ q_{JA}^\# R_A^\circ - 1 & q_{JA}^\# R_A^\circ \\ q_{AJ}^\# R_J^\circ + \pi_1^\circ q_{AA}^\# R_A^\circ & q_{AA}^\# R_A^\circ - 1 \end{pmatrix} = (0, 0) \quad (\text{A.25})$$

65 (where \mathbf{I} is the identity matrix), which explicitly (in elements) reads:

$$\underbrace{\ell_J^\circ (1 - q_{JJ}^\# R_J^\circ - \pi_1^\circ q_{JA}^\# R_A^\circ)}_{=1-a_{JJ}^\circ} = \ell_A^\circ (q_{AJ}^\# R_J^\circ + \pi_1^\circ q_{AA}^\# R_A^\circ), \quad (\text{A.26})$$

$$\underbrace{\ell_A^\circ (1 - q_{AA}^\# R_A^\circ)}_{=1-a_{AA}^\circ} = \ell_J^\circ q_{JA}^\# R_A^\circ. \quad (\text{A.27})$$

66 Using Eqns (A.26) and (A.27), we can now prove Eqn (A.15). Indeed, because the right-hand sides of
 67 Eqns (A.26) and (A.27) are both positive (by the Perron-Frobenius theorem), so are the left-hand sides of
 68 Eqns (A.26) and (A.27), implying that $1 - a_{JJ}^\circ > 0^2$ and $1 - a_{AA}^\circ > 0$ (remember the definition of a 's; see Eqn (A.13)).
 69 Under weak selection,

$$1 - a'_{JJ} + 1 - a'_{AA} = \underbrace{1 - a_{JJ}^\circ}_{>0} + \underbrace{1 - a_{AA}^\circ}_{>0} + \underbrace{(a_{JJ}^\circ - a'_{JJ}) + (a_{AA}^\circ - a'_{AA})}_{=\mathcal{O}(|\mathbf{v}' - \mathbf{v}|)}; \quad (\text{A.28})$$

70 where $\mathcal{O}(|\mathbf{v}' - \mathbf{v}|)$ represents the Landau's big- \mathcal{O} (for $|\mathbf{v}' - \mathbf{v}| \rightarrow 0$) such that the latter two terms both tend towards
 71 zero as $|\mathbf{v}' - \mathbf{v}| \rightarrow 0$. Since a'_{JJ} and a'_{AA} are both continuous functions of \mathbf{v}'^3 , under sufficiently weak mutation, we
 72 can assure the left-hand side of Eqn (A.28) be positive.

73 A.7 Selection gradient for juvenile virulence

74 In terms of q , R and π_1 , the invasion fitness reads:

$$w(\mathbf{v}', \mathbf{v}) = q_{JJ}^\# R_J' + \pi_1' q_{JA}^\# R_A' + q_{AA}^\# R_A' - q_{JJ}^\# q_{AA}^\# R_A' R_J' + q_{JA}^\# q_{AJ}^\# R_A' R_J'. \quad (\text{A.29})$$

75 Specifically, the fitness subcomponents involving v_J' amount to⁴:

$$\begin{aligned} w_J(v_J', v_J) &:= q_{JJ}^\# R_J' + \pi_1' q_{JA}^\# R_A^\circ - q_{JJ}^\# q_{AA}^\# R_A^\circ R_J' + q_{JA}^\# q_{AJ}^\# R_A^\circ R_J' \\ &= q_{JJ}^\# (1 - q_{AA}^\# R_A^\circ) R_J' + (\pi_1' + q_{AJ}^\# R_J') q_{JA}^\# R_A^\circ, \end{aligned} \quad (\text{A.30})$$

²This inequality consequently assures $1 - \frac{\alpha_J S_J^\# \sigma_{JJ} \beta_J^\circ}{H^\# \mu_J^\circ} = 1 - q_{JJ}^\# R_J^\circ > 0$ when $\rho \neq 1$.

³Note here that $S_J^\#$, $S_A^\#$, $I_J^\#$, and $I_A^\#$ are all independent of \mathbf{v}' because mutation is rare.

⁴Essentially, the invasion fitness subcomponents that do not contribute to the reproductive success of a parasite infecting a juvenile host are "excluded" from w_J .

76 which we have evaluated at $v'_A = v_A$. Since $q_{JA}^\# R_A^\circ = \ell_A^\circ / \ell_J^\circ (1 - q_{AA}^\# R_A^\circ)$, we finally have:

$$w_J(v'_J, v_J) = \left(1 - q_{AA}^\# R_A^\circ\right) \left(q_{JJ}^\# R_J' + \frac{\ell_A^\circ}{\ell_J^\circ} \cdot \left(\pi_1' + q_{AJ}^\# R_J' \right) \right) \quad (\text{A.31})$$

77 when $\rho \neq 1$.

78 This expression is easier to differentiate:

$$\begin{aligned} g_J(\mathbf{v}) &= \frac{1 - q_{AA}^\# R_A^\circ}{\ell_J^\circ} \cdot \left(\ell_J^\circ q_{JJ}^\# R_J^\circ \left(\frac{1}{\beta_J} \cdot \frac{d\beta_J}{dv_J} - \frac{1}{\mu_J} \right)^\circ + \ell_A^\circ q_{AJ}^\# R_J^\circ \left(\frac{1}{\beta_J} \cdot \frac{d\beta_J}{dv_J} - \frac{1}{\mu_J} \right)^\circ - \ell_A^\circ \pi_1^\circ \cdot \frac{1}{\mu_J} \right) \\ &= \frac{1 - q_{AA}^\# R_A^\circ}{\ell_J^\circ} \left(\left(\ell_J^\circ q_{JJ}^\# + \ell_A^\circ q_{AJ}^\# \right) \times R_J^\circ \left(\frac{1}{\beta_J} \cdot \frac{d\beta_J}{dv_J} - \frac{1}{\mu_J} \right)^\circ - \ell_A^\circ \pi_1^\circ \frac{1}{\mu_J} \right). \end{aligned} \quad (\text{A.32})$$

79 Using Eqn (A.27) to replace ℓ_A° (on the final factor) with $\left(\ell_J^\circ q_{JA}^\# + \ell_A^\circ q_{AA}^\# \right) R_A^\circ$ we get the selection gradient of
80 juvenile-virulence in the main text.

81 For the completeness, we can similarly get:

$$g_A(\mathbf{v}) = \left(1 - q_{JJ}^\# R_J^\circ\right) \left(q_{AA}^\# + \frac{\ell_J^\circ}{\ell_A^\circ} q_{JA}^\# \right) \frac{\beta_A}{\mu_A} \left(\frac{1}{\beta_A} \frac{d\beta_A}{dv_A} - \frac{1}{\mu_A} \right). \quad (\text{A.33})$$

82 Note that the first multiplicative term is always positive (see Footnote 2 and eqn (A.28)).

83 Using $\beta_A(v_A) = b_A k_A v_A / (1 + k_A v_A)$, it immediately follows that $g_A = 0$ is solved by $v_A^* = \sqrt{(m_A + \gamma_A) / k_A}$
84 and thus $v_A^* = \sqrt{m_A / k_A}$ in the absence of recovery ($\gamma_A = 0$).

85 A.8 Graph-theoretical approach

86 We here employ the graph-theoretical approach (GTA) developed by de Camino Beck & Lewis (2007), de
87 Camino Beck & Lewis (2008), and de Camino Beck *et al.* (2008) to derive the invasion fitness measure (SI Fig 2),
88 thereby checking the validity of $w(\mathbf{v}', \mathbf{v})$ in the main text. We write \mathcal{R}'_m for the invasion fitness derived through
89 GTA.

90 The premise of the approach is to decompose fecundity output and state-transitions as in the next-generation
91 theorem. The Jacobian around the endemic equilibrium reads:

$$\mathbf{J}' = \begin{pmatrix} q_{JJ}^\# \beta_J' - \mu_J' & q_{JA}^\# \beta_A' \\ u + q_{AJ}^\# \beta_J' & q_{AA}^\# \beta_A' - \mu_A' \end{pmatrix} = \begin{pmatrix} A'_{JJ} & A'_{JA} \\ A'_{AJ} & A'_{AA} \end{pmatrix}. \quad (\text{A.34})$$

92 de Camino Beck *et al.* (2008) defined three rules to algorithmically convert a compartmental structure into a
93 simplified model; partially borrowing the descriptions from de Camino Beck *et al.* (2008), we detail these as follows:

94 **Rule A: Self-loop elimination (trivialization)** To reduce the loop A'_{XX} (which is < 0) to -1 at node X, every arc
95 entering X has weight divided by $-A'_{XX} \mathcal{R}'_m$ (SI Fig 2A).

96 **Rule B: Parallel path elimination** For a path $X \rightarrow Y$, if the path includes two weights then these are merged with
 97 the weight given as the sum of the two weights (SI Fig 2B).

98 **Rule C: trivial node elimination** For a trivialized node Y on a path $X \rightarrow Y \rightarrow Z$, the two arcs are replaced by a
 99 single arc $X \rightarrow Z$ with weight equal to A'_{XY} times A'_{YZ} . Weights on multiple arcs $X \rightarrow Z$ are added. If there
 100 are no more paths through the trivial node Y , then it can be disregarded (SI Fig 2C).

101 Applying these rules, we can obtain the invasion condition, of:

$$\mathcal{R}'_m = \sqrt{\frac{\pi'_1 + q_{AJ}^\# R'_J}{1 - q_{JJ}^\# R'_J} \cdot \frac{q_{JA}^\# R'_A}{1 - q_{AA}^\# R'_A}}, \quad (\text{A.35})$$

102 with an elementary calculation showing $\mathcal{R}'_m > 1$ if and only if $w(\mathbf{v}', \mathbf{v}) > 1$ under weak selection. The expression
 103 in Eqn (A.35) indicates that the invasion fitness can be decomposed into juvenile and adult components. Choice
 104 of \mathcal{R}'_m , $w(\mathbf{v}', \mathbf{v})$, or $\Lambda[\mathbf{G}']$ is a matter of preference, all giving the same result for selection gradients and stability
 105 analyses. Taking advantage of deriving \mathcal{R}'_m (Eqn (A.35)), we can simplify the stability analysis (see the next
 106 subsection).

107 A.9 Attainability and Evolutionary stability

108 Here we outline the stability analyses for the evolutionary dynamics. Since the invasion fitness is not explicitly
 109 dependent on wild type strategy, the evolutionary stability and attainability conditions necessarily coincide (Otto
 110 & Day 2007). For this reason, we need only work on the evolutionary stability condition.

111 From Eqn (A.35), the invasion fitness is, in a product form, given by:

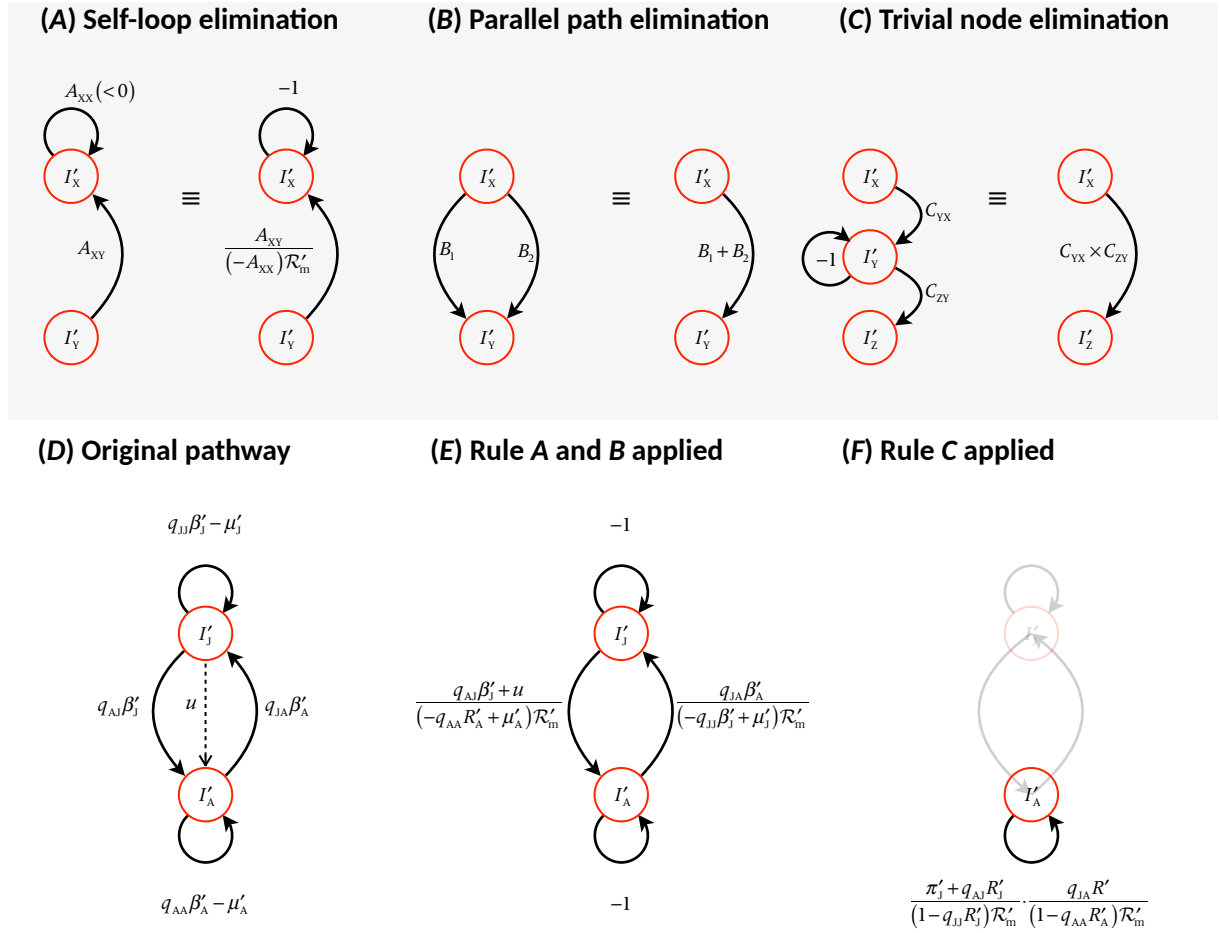
$$\mathcal{R}'_m(\mathbf{v}') = \sqrt{\mathcal{W}'_J(v'_J) \cdot \mathcal{W}'_A(v'_A)}, \quad (\text{A.36})$$

112 from which we can say that:

$$\begin{aligned} g_J &\propto \left(\frac{\partial \mathcal{W}'_J}{\partial v'_J} \right)^\circ, \\ g_A &\propto \left(\frac{\partial \mathcal{W}'_A}{\partial v'_A} \right)^\circ, \end{aligned} \quad (\text{A.37})$$

113 indicating that the Hessian matrix \mathcal{H} of \mathcal{R}'_m at SS be given as a diagonal matrix; indeed:

$$\mathcal{H} = \begin{pmatrix} \frac{\partial^2 \mathcal{R}'_m}{\partial v'^2_J} & \frac{\partial^2 \mathcal{R}'_m}{\partial v'_J \partial v'_A} \\ \frac{\partial^2 \mathcal{R}'_m}{\partial v'_A \partial v'_J} & \frac{\partial^2 \mathcal{R}'_m}{\partial v'^2_A} \end{pmatrix} = \begin{pmatrix} \mathcal{W}'_A \cdot \frac{\partial^2 \mathcal{W}'_J}{\partial v'^2_J} & \frac{\partial \mathcal{W}'_J}{\partial v'_J} \cdot \frac{\partial \mathcal{W}'_A}{\partial v'_A} \\ \frac{\partial \mathcal{W}'_J}{\partial v'_J} \cdot \frac{\partial \mathcal{W}'_A}{\partial v'_A} & \mathcal{W}'_J \cdot \frac{\partial^2 \mathcal{W}'_A}{\partial v'^2_A} \end{pmatrix}, \quad (\text{A.38})$$



SI Figure 2: Graph-theoretical reduction of reproductive success pathways. \mathcal{R}'_m represents the measure of invasion fitness; (A-C): general procedures in de Camino Beck & Lewis (2008). From this, by setting the last quantity unity, analytical expression of \mathcal{R}'_m derives. (D): The “original” diagram depicting the pathways of reproductive success. I'_j and I'_A both have self-loop, so we will apply “self-loop” elimination rule. In addition, we apply parallel path elimination rule (by summing the transition, u , and the reproductive success of parasites infecting juveniles to adults through transmission, W'_{Aj}), obtaining (E): besides two trivial edges (“-1”), two nodes loop mutually and we apply node elimination rule, ending up with (F): the reproductive success of parasites infecting adults, the total number of “secondary” infection by mutant parasites, with all possible transmission-pathways included.

114 which, evaluated at SS, gives a diagonal matrix because selection gradient vanishes at SS. Hence, it suffices to show
 115 that these diagonal terms – or the double partial derivatives – are both negative; that is, we shall show:

$$\begin{aligned} \left(\frac{\partial^2 \mathcal{W}'_J}{\partial v'_J{}^2} \right)^\circ &< 0, \\ \left(\frac{\partial^2 \mathcal{W}'_A}{\partial v'_A{}^2} \right)^\circ &< 0. \end{aligned} \tag{A.39}$$

116 [∴] First, Eqn (A.36) indicates:

$$\begin{aligned} \mathcal{W}'_J &= \frac{\pi'_I + q_{AJ}^\# R'_J}{1 - q_{JJ}^\# R'_J}, \\ \mathcal{W}'_A &= \frac{q_{JA}^\# R'_A}{1 - q_{AA}^\# R'_A}, \end{aligned} \tag{A.40}$$

117 which with straightforward calculations gives:

$$\left. \frac{\partial^2 \mathcal{W}'_A}{\partial v'_A{}^2} \right|_{\mathbf{v}=\mathbf{v}^*} = q_{JA}^* \times \left(\underbrace{\frac{\partial^2 R'_A}{\partial v'_A{}^2}}_{<0} \times (1 - q_{AA}^* R_A^*)^2 + 2 \underbrace{\left(\frac{\partial R'_A}{\partial v'_A} \right)^2}_{=0 \text{ at SS}} (1 - q_{AA}^* R_A^*) q_{AA}^* \right) < 0, \tag{A.41}$$

118 as desired; note that if $\rho = 1$ then this second derivative is always null at the SS, meaning that any mutants in v_A
 119 are selectively neutral at the SS.

120 Second, the first derivative of \mathcal{W}'_J (prior to being evaluated at SS) reads:

$$\begin{aligned} \frac{\partial \mathcal{W}'_J}{\partial v'_J} &= \frac{1}{(1 - q_{JJ}^\# R'_J)^2} \left\{ (\pi_I^{[1]} + q_{AJ}^\# R_J^{[1]}) (1 - q_{JJ}^\# R'_J) + q_{JJ}^\# R_J^{[1]} (\pi'_I + q_{AJ}^\# R'_J) \right\} \\ &= \left\{ (\pi_I^{[1]} + q_{AJ}^\# R_J^{[1]}) (1 - q_{JJ}^\# R'_J) + q_{JJ}^\# R_J^{[1]} (\pi'_I + q_{AJ}^\# R'_J) \right\} (1 - q_{JJ}^\# R'_J)^{-2} \end{aligned} \tag{A.42}$$

121 (with the shorthand notation $^{[1]}$ for its first derivative with respect to v'_J), from which, as the selection gradient $g_J(\mathbf{v})$
 122 vanishes at \mathbf{v}^* , we have:

$$\left(\pi_I^\circ q_{JJ}^\# + q_{AJ}^\# \right) \left(R_J^{[1]} \right)^\circ = - \left(\pi_I^{[1]} \right)^\circ (1 - q_{JJ}^\# R'_J). \tag{A.43}$$

¹²³ Also, using $R'_J = \beta'_J / \mu'_J$, we immediately have:

$$\begin{aligned} (R_J^{[1]})^\circ &= \left(\frac{dR'_J}{dv'_J} \right)^\circ = \left(\frac{\beta_J^{[1]} \mu_J - \beta_J}{\mu_J^2} \right)^\circ, \\ (R_J^{[2]})^\circ &= \left(\frac{d^2 R'_J}{dv'^2_J} \right)^\circ = \left(\frac{\beta_J^{[2]}}{\mu_J} - \frac{2}{\mu_J} R_J^{[1]} \right)^\circ. \end{aligned} \quad (\text{A.44})$$

¹²⁴ The second derivative of \mathcal{W}'_J evaluated at SS reads:

$$\begin{aligned} \left. \frac{\partial^2 \mathcal{W}'_J}{\partial v'^2_J} \right|_{\mathbf{v}=\mathbf{v}^*} &= \left\{ \pi_1^{[2]} (1 - q_{JJ}^* R_J^*) + \pi_1^{[1]} (-q_{JJ}^* R_J^{[1]}) + q_{AJ}^* R_J^{[2]} + q_{JJ}^* R_J^{[2]} \pi_1 + q_{JJ}^* R_J^{[1]} \pi_1^{[1]} \right\}^* \cdot (1 - q_{JJ}^* R_J^*)^{-2} \\ &\quad + 2q_{JJ}^* (R_J^{[1]})^* \cdot (1 - q_{JJ}^* R_J^*)^{-3} \cdot \underbrace{\left\{ (\pi_1^{[1]} + q_{AJ}^* R_J^{[1]}) (1 - q_{JJ}^* R_J^*) + q_{JJ}^* R_J^{[1]} (\pi_1^* + q_{AJ}^* R_J^*) \right\}^*}_{\propto g_J(\mathbf{v}^*)=0 \text{ at SS}} \\ &= \left\{ \pi_1^{[2]} (1 - q_{JJ}^* R_J^*) + q_{AJ}^* R_J^{[2]} + q_{JJ}^* R_J^{[2]} \pi_1 \right\}^* \cdot (1 - q_{JJ}^* R_J^*)^{-2} \end{aligned} \quad (\text{A.45})$$

¹²⁵ As $\pi_1 = u/(u + m_J + v_J)$, the first and second derivatives at SS are given by:

$$(\pi_1^{[1]})^\circ = - \left(\frac{\pi_1}{\mu_J} \right)^\circ, \quad (\text{A.46})$$

$$(\pi_1^{[2]})^\circ = \left(\frac{2\pi_1}{(\mu_J)^2} \right)^\circ, \quad (\text{A.47})$$

126 which, plugged into Eqn (A.45), give:

$$\begin{aligned}
\left. \frac{\partial^2 \mathcal{W}'_J}{\partial v_J^2} \right|_{\mathbf{v}^*} &= \left\{ \pi_1^{[2]} (1 - q_{JJ}^\# R_J) + q_{AJ}^\# R_J^{[2]} + q_{JJ}^\# R_J^{[2]} \pi_1 \right\}^\circ \cdot (1 - q_{JJ}^\# R_J^\circ)^{-2} \\
&= \left\{ \pi_1^{[2]} (1 - q_{JJ}^\# R_J) + (\pi_1 q_{JJ}^\# + q_{AJ}^\#) \underbrace{R_J^{[2]}}_{\text{use Eqn (A.44)}} \right\}^\circ \cdot (1 - q_{JJ}^\# R_J^\circ)^{-2} \\
&= \left\{ \underbrace{\pi_1^{[2]}}_{\text{use Eqn (A.47)}} (1 - q_{JJ}^\# R_J) + (\pi_1 q_{JJ}^\# + q_{AJ}^\#) \left(\frac{\beta_J^{[2]}}{\mu_J} - \frac{2}{\mu_J} R_J^{[1]} \right) \right\}^\circ \cdot (1 - q_{JJ}^\# R_J^\circ)^{-2} \\
&= \left\{ \frac{2\pi_1}{(\mu_J)^2} (1 - q_{JJ}^\# R_J) + (\pi_1 q_{JJ}^\# + q_{AJ}^\#) \left(\frac{\beta_J^{[2]}}{\mu_J} - \underbrace{\frac{2}{\mu_J} R_J^{[1]}}_{\text{use Eqn (A.44)}} \right) \right\}^\circ \cdot (1 - q_{JJ}^\# R_J^\circ)^{-2} \tag{A.48} \\
&= \left\{ \frac{2\pi_1}{(\mu_J)^2} (1 - q_{JJ}^\# R_J) + (\pi_1 q_{JJ}^\# + q_{AJ}^\#) \left(\frac{\beta_J^{[2]}}{\mu_J} \right) + \underbrace{\frac{2\pi_1^{[1]}}{\mu_J}}_{=-2\pi_1/\mu_J^2} (1 - q_{JJ}^\# R_J) \right\}^\circ \cdot (1 - q_{JJ}^\# R_J^\circ)^{-2} \\
&= \underbrace{(\pi_1^\circ q_{JJ}^\# + q_{AJ}^\#)}_{>0} \underbrace{\left(\frac{\beta_J^{[2]}}{\mu_J} \right)^\circ}_{<0} \cdot (1 - q_{JJ}^\# R_J^\circ)^{-2} < 0,
\end{aligned}$$

127 which completes the proof of the statement Eqn (A.39).

128 A.10 Condition for parasite persistence

129 In the absence of diseases,

$$\begin{aligned}
\frac{dS_J}{dt} &= (r - \kappa S_A) \cdot S_A - (u + m_J) S_J, \\
\frac{dS_A}{dt} &= u S_J - m_A S_A.
\end{aligned} \tag{A.49}$$

130 Disease-free equilibrium is given by:

$$(S_J, S_A) = (S_J^{(0)}, S_A^{(0)}) = \left(\frac{m_A}{u} \cdot \frac{r - m_A \frac{u + m_J}{u}}{\kappa}, \frac{r - m_A \frac{u + m_J}{u}}{\kappa} \right), \quad (\text{A.50})$$

131 from which we can get:

$$\frac{S_A^{(0)}}{S_J^{(0)} + S_A^{(0)}} = \frac{u}{u + m_A}. \quad (\text{A.51})$$

132 Parasites attempting to invade such a disease-free, stage-structured host population can establish only if:

$$R_0 = \alpha_J \frac{m_A}{u + m_A} \sigma_{JJ} \frac{\beta_J}{\mu_J} + \frac{u}{\mu_J} \cdot \alpha_J \frac{m_A}{u + m_A} \sigma_{JA} \frac{\beta_A}{\mu_A} + \alpha_A \frac{u}{u + m_A} \sigma_{AA} \frac{\beta_A}{\mu_A} - \alpha_J \alpha_A \rho \cdot \frac{u}{u + m_A} \cdot \frac{m_J}{u + m_A} \cdot \frac{\beta_J \beta_A}{\mu_J \mu_A} > 1. \quad (\text{A.52})$$

133 When the outcomes of selection (i.e., $(v_J, v_A) = (v_J^*, v_A^*)$) violate this condition, parasite extinction (evolutionary
134 suicide) can occur.

135 A.11 When $\rho = 1$ (fully assortative transmission)

136 Finally, we detail what if $\rho = 1$; then $\Lambda[\mathbf{G}']$ is given by:

$$\Lambda[\mathbf{G}'] = \max \left(q_{JJ}^{\#} R'_J, q_{AA}^{\#} R'_A \right) = \max \left(\frac{R'_J}{R_J}, \frac{R'_A}{R_A} \right) \quad (\text{A.53})$$

137 In this case, obtaining the selection gradient is not needed. Instead, we can directly see that the evolutionary stability
138 condition reads:

$$\max \left(q_{JJ}^{\#} R'_J, q_{AA}^{\#} R'_A \right) = \max \left(\frac{R'_J}{R_J}, \frac{R'_A}{R_A} \right) < 1 \quad (\text{A.54})$$

139 for any $\mathbf{v}' \neq \mathbf{v}$. This is thus obtained by jointly maximizing two functions $R'_J = \beta_J(v'_J)/\mu'_J$ and $R'_A = \beta_A(v'_A)/\mu'_A$,
140 giving the CSS as $(v_J^*, v_A^*) = (\sqrt{(m_J + u)/k_J}, \sqrt{(m_A/k_A)})$.

141 B Robustness

142 In the main text, we have assumed:

- 143 • There is no recovery: $\gamma_J = \gamma_A = 0$;
- 144 • Susceptibility is the same: $\alpha_J = \alpha_A = 1$;
- 145 • Maximum infectiousness is the same: $b_J = b_A = 10$;
- 146 • The response of infectiousness to increased virulence (i.e., the efficiency improved growth due to exploitation)
147 is the same: $k_J = k_A = 1$;

148 • Transmission is frequency-dependent: $\phi_{XY} = \alpha_X \sigma_{XY} \beta_Y I_Y / H^\#$.

149 • Fecundity is the same for susceptible and infected adults.

150 Here we will check the robustness of our prediction against these variants. Specifically, we will work on the
151 specificity in:

152 • recovery: (γ_J, γ_A) ;

153 • susceptibility: (α_J, α_A) ;

154 • tolerance: (k_J, k_A) ;

155 • resistance: (b_J, b_A) ;

156 • density-dependent transmission: $\phi_{XY} = \alpha_X \sigma_{XY} \beta_Y I_Y$.

157 • fecundity changes in infected adults, $1 - h$ (with h possibly negative).

158 Note that we did not always show the full range of $\rho \in [-1, 1]$ and $\theta_A \in [0, 1]$, because the numerical routines
159 are computationally expensive. Also, we used the default parameter values unless otherwise specified; specifically,
160 $m_J = m_A = 1$.

161 B.1 Recovery

162 We used relatively small values of (γ_J, γ_A) in the ODE, because high recovery can readily result in parasite
163 extinction. We again numerically obtained the CSS virulence and plotted them on the (ρ, θ_A) -plane. We can see that
164 our prediction is qualitatively robust against this variant. Quantitative differences are that recovery can in general
165 favour fast exploitation, which is obvious from the CSS for adult virulence, $v_A^* = \sqrt{(m_A + \gamma_A)/k_A} > \sqrt{m_A/k_A}$.
166 In the numerical example, $\gamma_A = 0.25, k_A = m_A = 1$ yields $v_A^* = \sqrt{5}/2 \approx 1.118$. As for juvenile virulence v_J^* , the
167 general trend is unchanged (SI Fig 5).

168 As recovery increases, evolutionary suicide is more readily to occur (white zone). This is so because parasites
169 have to faster exploit the hosts while there is no trade-off between recovery and other traits (i.e., other traits do not
170 compensate the decreased infectious period).

171 Overall, the effects of recovery are similar to those of mortality (see Figure 2 in the main text).

172 B.2 Susceptibility

173 We here introduce a difference in α 's, which corresponds to the situation where juveniles and adults show
174 quantitatively different transmission-blocking mechanisms. This does not affect the results critically; a difference
175 is that evolutionary suicide is more likely to occur with smaller α 's.

176 B.3 Tolerance

177 Tolerance, or reduced negative impacts of the disease on hosts, can affect the tradeoff through k_X . For
178 simplicity, we assume that b_X is constant (see next section). To incorporate tolerance, we further decompose
179 parasite-induced mortality into $v_X = (1 - \tau_X) e_X$, where τ_X tunes tolerance and e_X represents exploitation.

180 Infectiousness-exploitation tradeoff can be given by:

$$\begin{aligned}\beta_X(e_X) &= b_X \frac{k_X e_X}{1 + k_X e_X} \\ &= b_X \frac{\frac{k_X}{1-\tau_X} v_X}{1 + \frac{k_X}{1-\tau_X} v_X},\end{aligned}\tag{B.55}$$

181 whereas a derivative is given by:

$$\frac{dv_X}{de_X} = 1 - \tau_X,\tag{B.56}$$

182 which is a constant for each X (with X = J or A). Higher tolerance (larger τ_X) leads to larger $k_X/(1 - \tau_X)$.

183 Marginal value theorem (Charnov 1976) shows that SS solves:

$$\frac{1}{\beta_A} \cdot \frac{d\beta_A}{de_A} = \frac{1 - \tau_A}{(1 - \tau_A)e_A + m_A},\tag{B.57}$$

184 supplying $e_A^* = \sqrt{m_A(1 - \tau_A)/k_A}$. Hence SS for e_A is smaller with tolerance. To look at the consequences for e_J ,
185 we again solved the equations, observing that the results are qualitatively unchanged.

186 B.4 Infectiousness

187 We assess the effects of varying b_X . Obviously, increasing b_X results in higher transmission but does not affect
188 the SS for adult virulence (SI Fig 6).

189 B.5 Density-dependent transmission

190 Because the densities would be of greater importance to the force of infection with this assumption, we used a
191 smaller value of $b_J = b_A = 0.13$. We found quantitatively similar outcomes (SI Fig 7).

192 B.6 Fecundity virulence and evolutionarily stable resource shifts

193 We here explore the effects of fecundity shifts on evolution of virulence, looking at the possibility that parasites
194 deprive some amounts of resource of infected hosts that would have been otherwise available to the hosts for
195 reproduction. We do so by considering two models: in the first model, we assume that the fecundity shift in
196 adults, denoted h , is a constant (h can be negative). We consequently found that the results are robust.

197 C Generalized pathway structure

198 In the main text we posed three constraints, namely normalization ($\sigma_{JA} + \sigma_{AA} = 1$ and $\sigma_{AJ} + \sigma_{JJ} = 1$) and
199 symmetry ($\sigma_{AJ} = \sigma_{JA}$), thereby tuning a single parameter of the diagonal element ($\sigma_{JJ} = \sigma_{AA} = \sigma$ was the
200 parameter of interest). Here we relax each of these assumptions, which we found did not dramatically change our
201 predictions.

202 We first of all remark that transmission terms are governed by four compound quantities ϕ_{XY} (with
 203 X and Y running across J and A), meaning that eight (or two pairs of four) multiplicative terms for
 204 $\alpha_J, \alpha_A, b_J, b_A, \sigma_{JJ}, \sigma_{AJ}, \sigma_{JA}, \sigma_{AA}$ are redundant; we can impose four constraints to these parameters. For instance,
 205 the condition $\sigma_{AA} = 1 \gg \sigma_{JJ} = 1/100$ with $\sigma_{JA} = \sigma_{AJ} = 1/2$ with $\alpha_J = \alpha_A = 1$ and $b_J = b_A = 10$ (such that
 206 pathway is symmetric), is equivalent to $\sigma_{AA} = 2/3, \sigma_{JA} = 1/3, b_A = 15, \sigma_{AJ} = 50/51, \sigma_{JJ} = 1/51, b_J = 51/10$
 207 (such that, with $\sigma_{AJ} + \sigma_{JJ} = \sigma_{AA} + \sigma_{JA} = 1$, the pathway pattern is normalized). The product-decomposition of the
 208 force of infection ϕ_{XY} is thus not unique. Therefore, as we have already shown that neither does a slight difference
 209 in susceptibility $\alpha_J \neq \alpha_A$ or in infectiousness $b_A \neq b_A$ affect the results, we can restrict ourselves to $\alpha_J = \alpha_A$ and
 210 $b_J = b_A$ (with two parameters reduced).

211 We further impose more constraints. In the first case, we assume $\sigma_{JJ} = 1 - \sigma_{AJ}$ and $\sigma_{AA} = 1 - \sigma_{JA}$ (normalized
 212 pathway) and varying σ_{JJ} and σ_{AA} ; the second is to fix σ_{AA} and vary σ_{JJ} and $\sigma_{JA} = \sigma_{AJ}$ (symmetric pathway).

213 **“Normalized pathway” : varying $\sigma_{JJ} = 1 - \sigma_{AJ}$ and $\sigma_{AA} = 1 - \sigma_{JA}$**

214 The pathway matrix reads

$$\begin{pmatrix} \sigma_{JJ} & 1 - \sigma_{JJ} \\ 1 - \sigma_{AA} & \sigma_{AA} \end{pmatrix}, \quad (\text{C.58})$$

215 with $\rho = \sigma_{JJ} + \sigma_{AA} - 1 \in [-1, 1]$. SI Fig 9 suggests that when θ_A is small, higher assortativity (top right zone)
 216 favors higher juveniles virulence (top panels) but this trend turns over as θ_A becomes larger.

217 **“Symmetric pathway” : varying σ_{JJ} and $\sigma_{AJ} = \sigma_{JA}$, with σ_{AA} fixed**

218 The pathway matrix reads

$$\begin{pmatrix} \sigma_{JJ} & \sigma_{AJ} \\ \sigma_{AJ} & \sigma_{AA} \end{pmatrix}, \quad (\text{C.59})$$

219 with $\rho = \sigma_{JJ} \cdot \sigma_{AA} - \sigma_{AJ}^2 \in [-1, 1]$. SI Fig 10 shows that, when θ_A is small (or large), smaller (or larger) σ_{AJ} favors
 220 higher juvenile-virulence (respectively). Therefore, the transmission pathway interpretation is again consistent and
 221 thus robust to this variant.

222 D Empirical data figure and credits

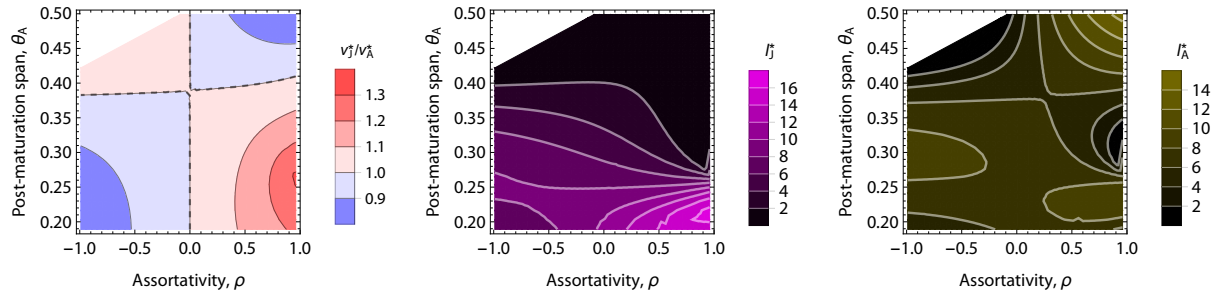
223 We conducted several literature searches in Google Scholar combining the terms “age- related” or
 224 “age-dependent” or “stage-dependent” or “juvenile” + “susceptibility” or “resistance” or “tolerance” or
 225 “immunocompetence” + “infection” or “infectious disease”. From these searches, we collected data from papers
 226 where the parasite could be judged to be adapted to its host (i.e., not a recent host shift and without significant multi-
 227 species transmission) and where differences in virulence across life stages could be distinguished from age-related
 228 trends in additional mortality due to increasing adaptive immunity with age due to previous exposure and increased
 229 mortality of poor-condition hosts during the juvenile stages. Therefore, we collected data from papers for host-

230 pathogen systems where adaptive immunity to the pathogen was not significant or infection-related mortality was
231 measured in naïve juveniles and adults in either a natural population or in an experimental lab population. From
232 the papers that we found, we also searched their citations and papers that cited them for other publications that we
233 may have missed in the first search. After we had found papers with reliable data on age- biased virulence, we
234 searched for “host” and “life history” or “age at reproduction” to find data on the host’s maturation rate. Finally, we
235 searched for transmission assortativity data for each selected system by searching the terms “host”+ “transmission”
236 or “contact network”+ “age” or “stage” or “juvenile”. We used estimated values of v_J versus v_A . The extracted
237 data are plotted against a (ρ, θ_A) -plane.

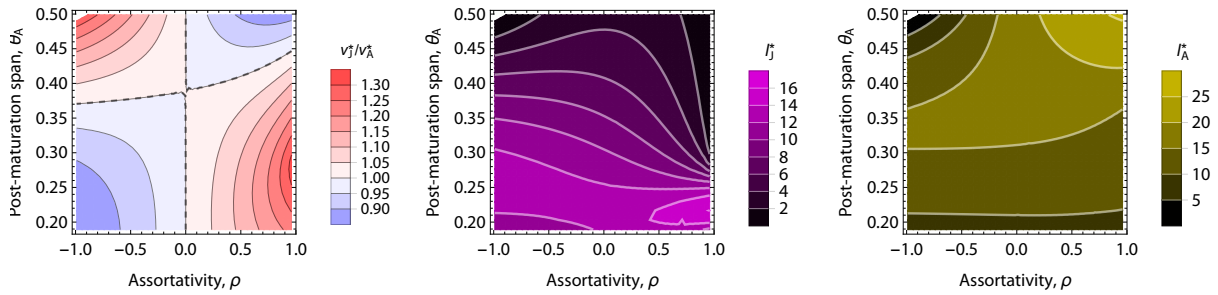
238 Concerning the data on asian elephants (*Elephas maximus*), we assessed the relative virulence v_J/v_A from the
239 published literature (Lynsdale *et al.* 2017) as well as personal communication with C. Lynsdale and V. Lummaa.
240 The censused individuals (in total 4242) are categorized into reproductives (aged 8 or above; 3046 individuals)
241 and non-reproducible (under 8; 1196 individuals) (c.f. Sukumar *et al.* 1997). Parasite-caused and potentially
242 parasite-associated deaths, in total, occurred in 304 reproductives or in 301 non-reproductives, each among which
243 parasite-caused death was identified as 85 for reproductives or 91 for non-reproductives, respectively (we thank
244 C. Lynsdale and V. Lummaa for sharing the data of stage-specific mortality). However, we were unable to assess
245 the virulence values for this data, due to a lack of information on stage-specific prevalence or proportion of infected
246 individuals at the time of death or censorship. Therefore, we restricted ourselves to citing the evidence that
247 extremely young individuals are at higher risk of parasite-induced death (see Figure2 in Lynsdale *et al.* 2017).
248 We propose that future studies quantifying stage-dependent parasite prevalence is greatly promising to test our
249 predictions.

250 All drawings were downloaded from [PhyloPic](#). Credits: (a) Uncredited; (b) [David Liao](#), under [CC BY-SA 3.0](#);
251 (c, d) Both uncredited; (e) [T. Michael Keeseey](#), under [CC BY 3.0](#) (the image has been reflected from original); (f)
252 Uncredited; (g) [Anthony Caravaggi](#), under [CC BY-NC-SA 3.0](#) (the image has been reflected from original); (h) [Luc](#)
253 [Viatour](#) (source photo) and [Andreas Plank](#), under [CC BY-SA 3.0](#).

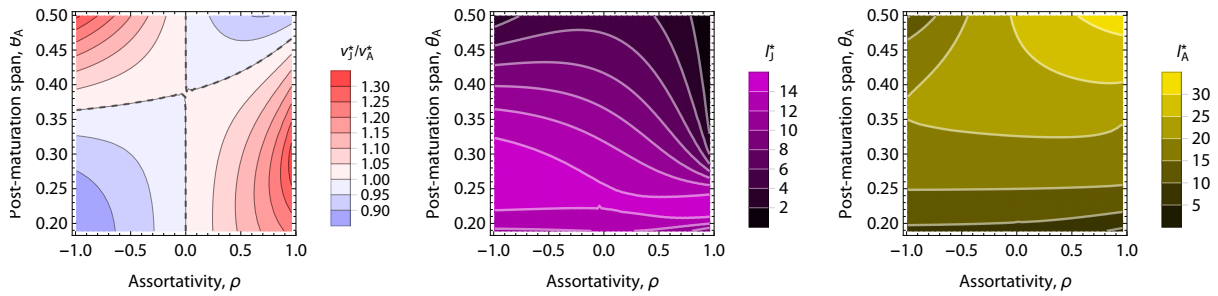
(A) $\alpha_j=1, \alpha_A=0.75$



(B) $\alpha_j=1, \alpha_A=1$

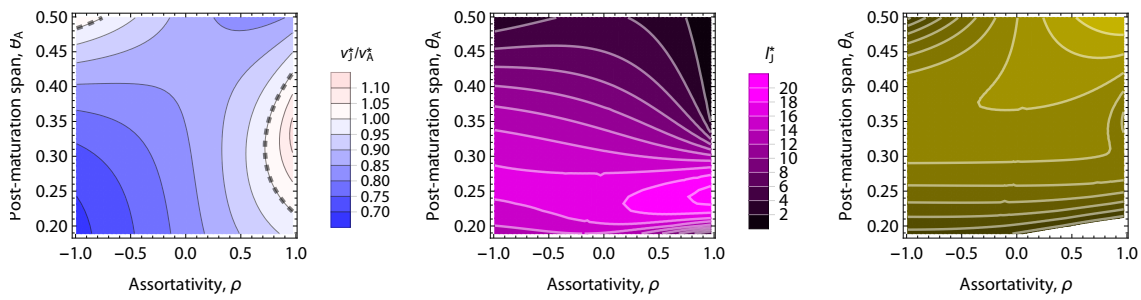


(C) $\alpha_j=1, \alpha_A=1.25$

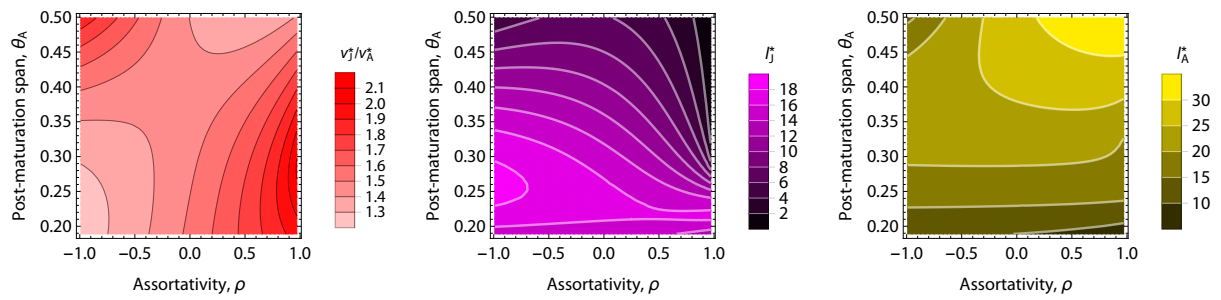


SI Figure 3: Effects of varying susceptibility. Changes in susceptibility have minor effects on the CSS (left panels), whereas evolutionary suicide is more likely to occur with smaller susceptibility (panel A's).

(A) $\tau_J=0.375, \tau_A=0$.

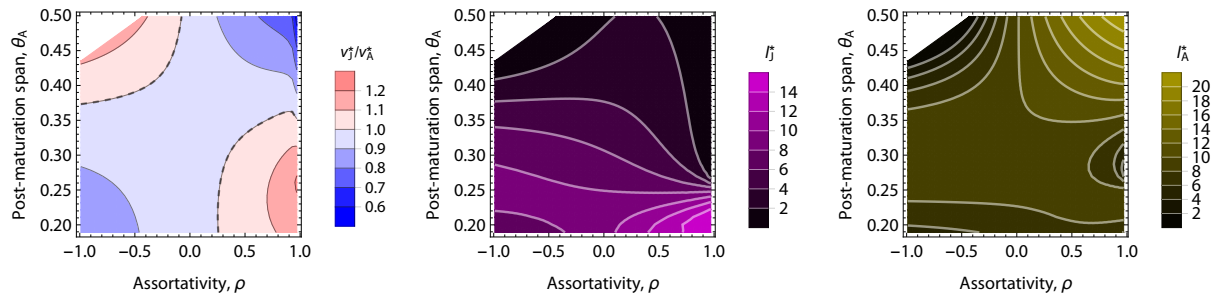


(B) $\tau_J=0, \tau_A=0.375$

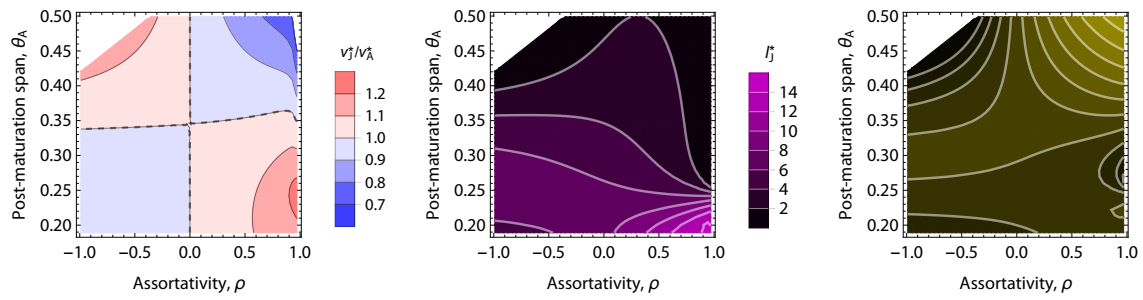


SI Figure 4: Effects of varying tolerance. Tolerance in adults can lead to relatively higher virulence for juveniles; note that $v_A^* = \sqrt{m_A(1 - \tau_A)/k_A}$ is dependent on τ_A . Due to the tolerance, the number of infected adults increase with h_A . Overall, the qualitative trend is unchanged.

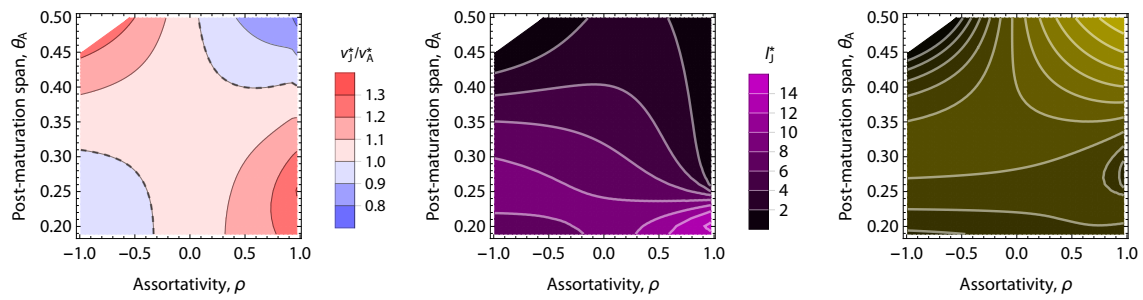
(A) $\gamma_J=0.125, \gamma_A=0.25$



(B) $\gamma_J=0.25, \gamma_A=0.25$

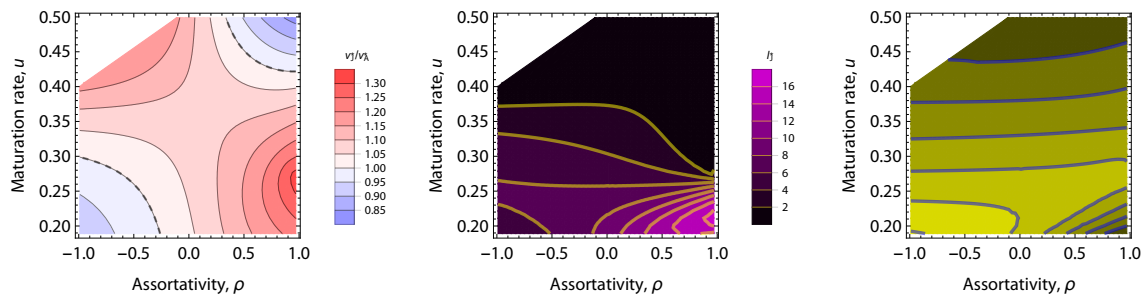


(C) $\gamma_J=0.25, \gamma_A=0.125$

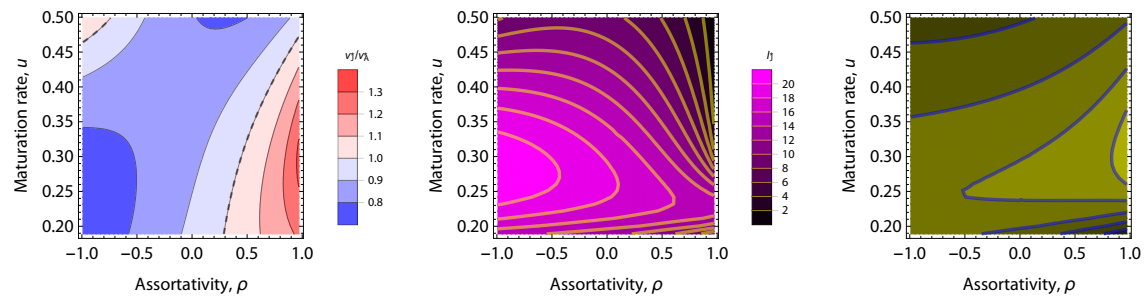


SI Figure 5: Effects of varying recovery rates. The results are quantitatively unchanged, but evolutionary suicide is more likely to occur (white zone). Dashed contours: $v_J^* = v_A^*$. Default values were used for other parameters (main text).

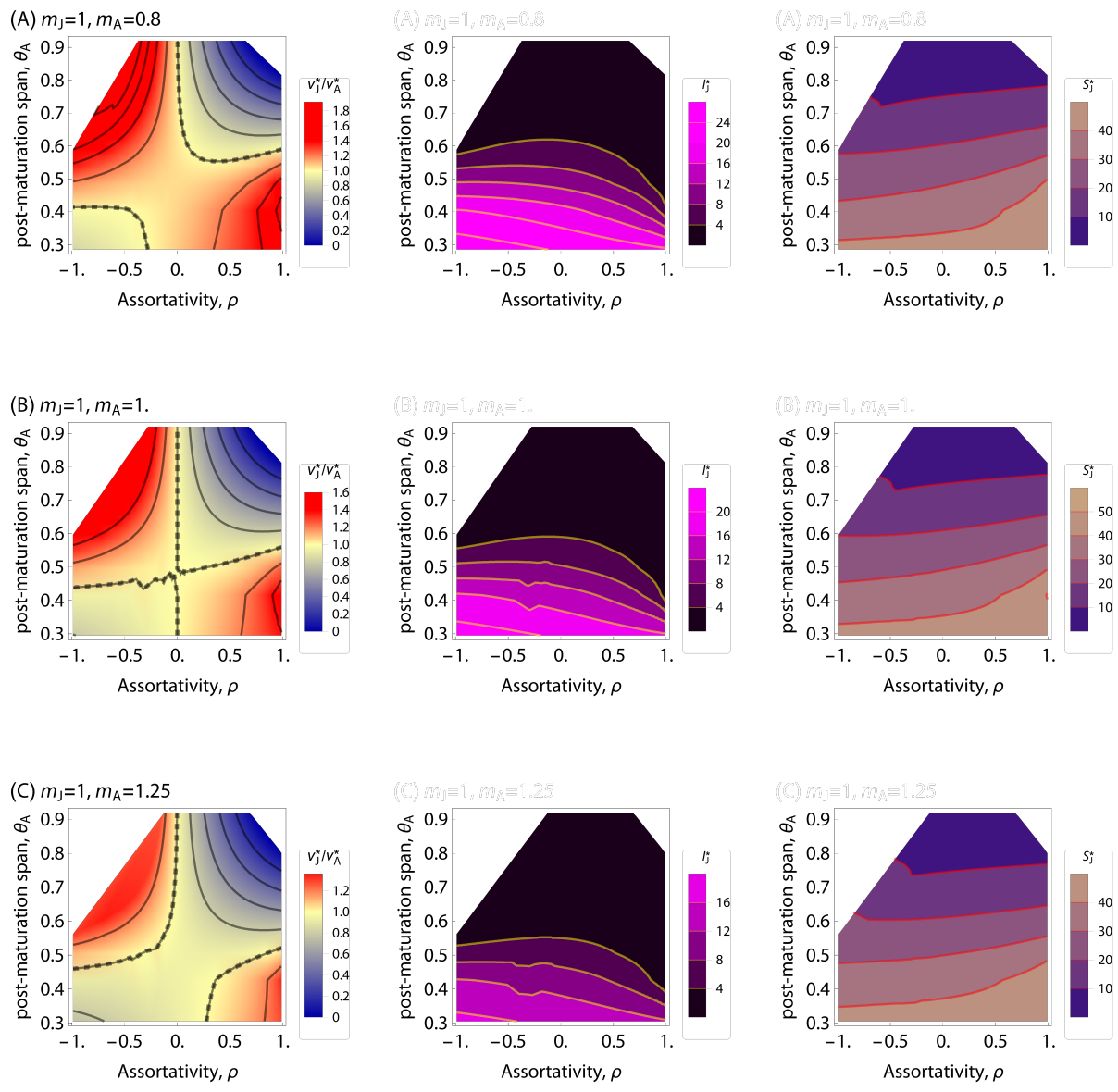
(A) $b_J=10, b_A=8$.



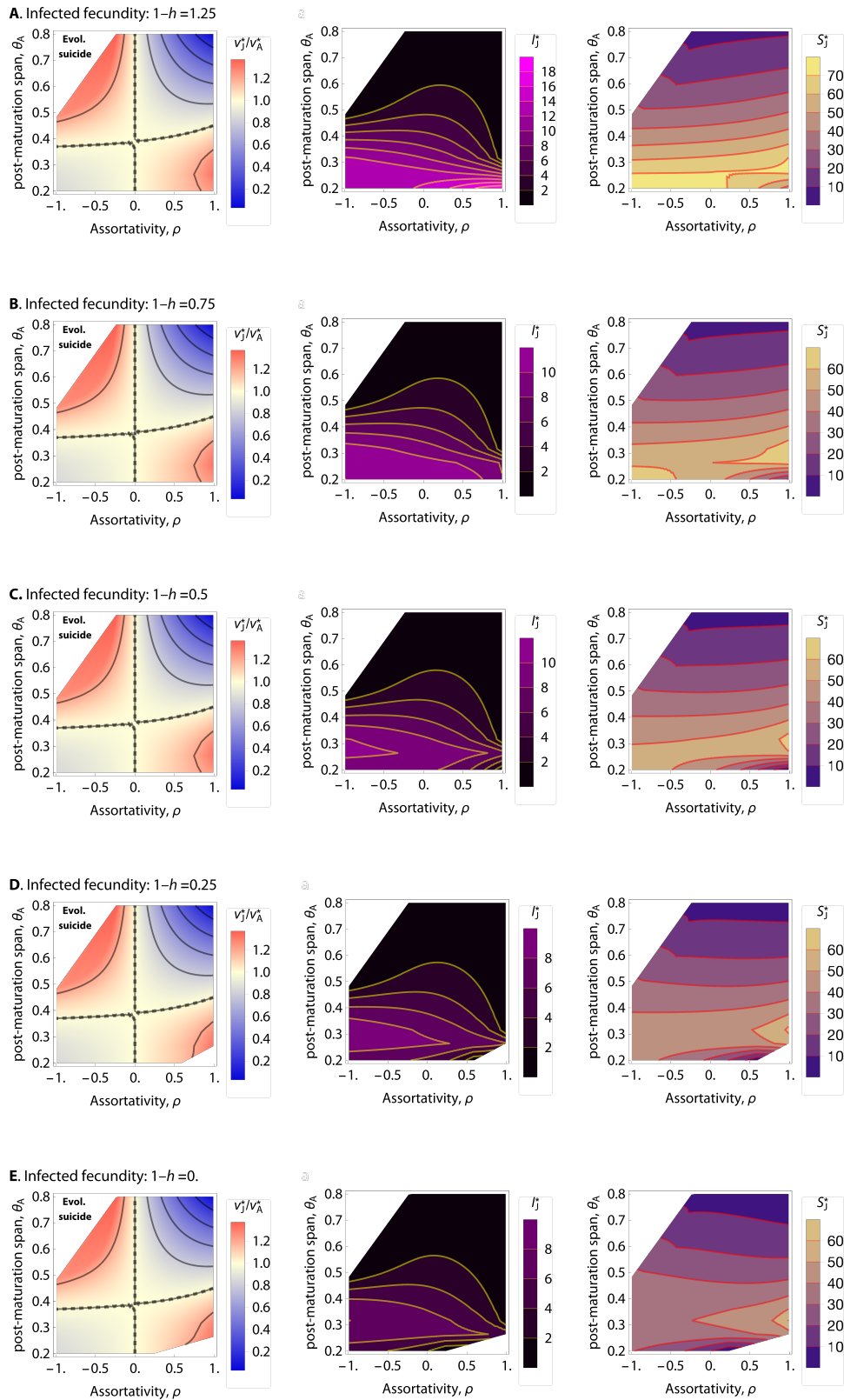
(B) $b_J=10, b_A=14$.



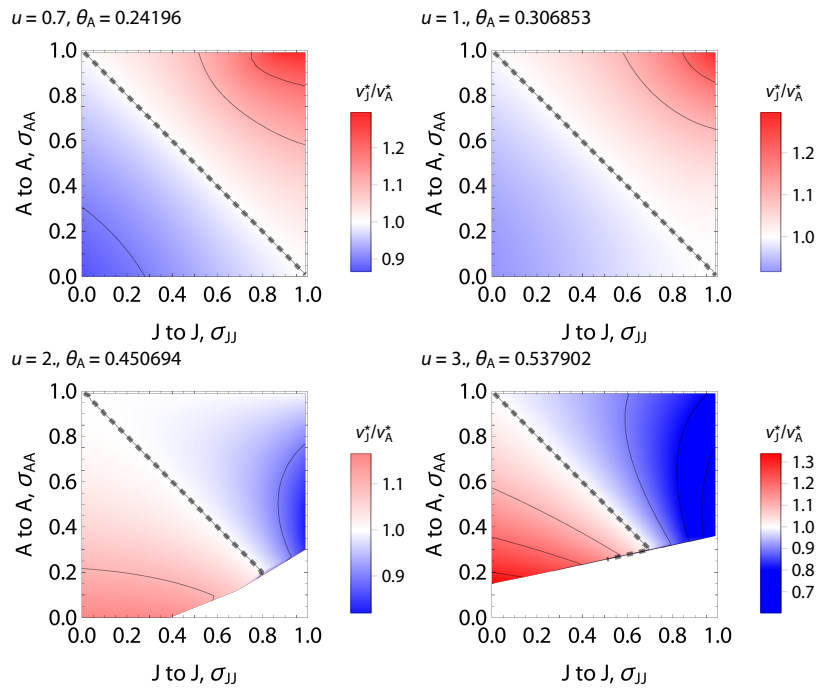
SI Figure 6: Effects of varying infectiousness. Different infectiousness can lead to higher virulence for juveniles; note that $v_A^* = \sqrt{m_A/k_A}$ is independent of b_A and b_J . Overall, the qualitative trend is unchanged, but the disease prevalence among juveniles is dramatically lower with assortativity.



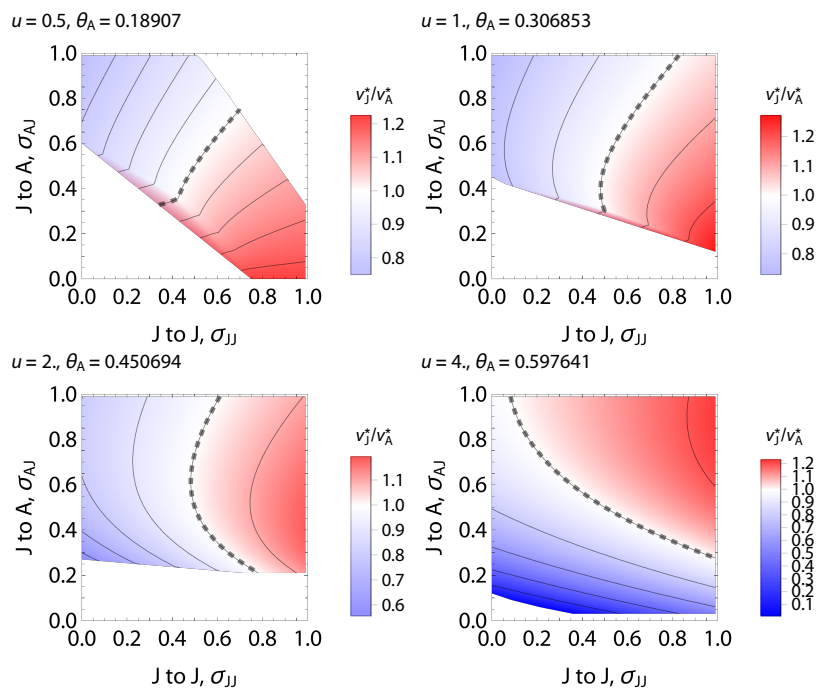
SI Figure 7: Effects of density-dependence.



SI Figure 8: Effects of constant fecundity virulence. The factor $1 - h$ measuring the fecundity of infected adults. The resulting difference is minor, as fecundity reduction acts only via ecological feedback without any direct effects on the invasion fitness. Also note that in panel (A), the fecundity is higher for infected than for susceptible adults.



SI Figure 9: Effects of the normalized pathway structure, with $\sigma_{JA} = 1 - \sigma_{AA}$ and $\sigma_{AJ} = 1 - \sigma_{JJ}$. Orthogonal dashed line, which satisfies $\rho = \sigma_{JJ} + \sigma_{AA} - 1 = 0$, gives $v_j^* = v_A^*$. Note, we fixed $m_J = m_A = 1$, and thus θ_A is a function of u (e.g., $u = 1$ gives $\theta_A = 0.306853$).



SI Figure 10: Effect of the symmetric pathway structure, with $\sigma_{JA} = \sigma_{AJ}$ varied and $\sigma_{AA} = 0.5$ fixed. Note that fixing u determines a single value of θ_A , and for clarity we have shown both of the values (u and θ_A).

SI Table: Data on empirical host-parasite systems.

Host	Parasites	vJ/vA	Adult Period	Assortativity	Refs
Pink salmon (<i>Oncorhynchus gorbuscha</i>)	Salmon Louse	>1	≈0 (semelparity)	Assortative	Heard 1991; Jones <i>et al.</i> 2008
Gerbil (<i>Gerbillus andersoni</i>)	Ectoparasites	1.79	0.41	-	Wassif & Soliman 1980; Delany 1986; Hawlena <i>et al.</i> 2006
Fruit fly (<i>Drosophila melanogaster</i>)	Bacteria (<i>Pseudomonas entomophila</i>)	1.43	0.63	-	Vodovar <i>et al.</i> 2005; Luckinbill <i>et al.</i> 1984
Common guillemot (<i>Uria aalge</i>)	Great Island Virus	0.69	0.70	Assortative	Harris & Wanless 1995; Nunn <i>et al.</i> 2006; Wanelik <i>et al.</i> 2017
Asian elephant (<i>Elephas maximus</i>)	Parasites	>1	0.76	-	Sukumar <i>et al.</i> 1997; Lynsdale <i>et al.</i> 2017
European rabbit (<i>Oryctolagus cuniculus</i>)	Nematode	1.00	0.83	-	von Holst <i>et al.</i> 2002; Cornell <i>et al.</i> 2008
Rabbits (<i>Leporidae</i>)	RHD Virus	0.67	0.83	-	Morisse <i>et al.</i> 1991; Reluga <i>et al.</i> 2007
Pigeon (<i>Columba livia</i>)	Blood Parasite	1.85	0.92	-	Lack 1968; Holmes & Ottinger 2003; Sol <i>et al.</i> 2003

References

- 255
- 256 Caswell, H. (2001). *Matrix population models*. Wiley Online Library.
- 257 Charnov, E. L. (1976). Optimal foraging, the marginal value theorem. *Theoretical Population Biology* **9**.2,
258 pp. 129–136.
- 259 de Camino Beck, T. & Lewis, M. A. (2007). A new method for calculating net reproductive rate from graph reduction
260 with applications to the control of invasive species. *Bulletin of Mathematical Biology* **69**.4, pp. 1341–1354. DOI:
261 [10.1007/s11538-006-9162-0](https://doi.org/10.1007/s11538-006-9162-0).
- 262 — (2008). On Net Reproductive Rate and the Timing of Reproductive Output. *The American Naturalist* **172**.1,
263 pp. 128–139. DOI: [10.1086/588060](https://doi.org/10.1086/588060).
- 264 de Camino Beck, T., Lewis, M. A., & van den Driessche, P. (2008). A graph-theoretic method for the basic
265 reproduction number in continuous time epidemiological models. *Journal of Mathematical Biology* **59**.4,
266 pp. 503–516. DOI: [10.1007/s00285-008-0240-9](https://doi.org/10.1007/s00285-008-0240-9).
- 267 Fisher, R. A. (1958). *The genetical theory of natural selection*. Tech. rep. Dover Publications,
- 268 Frank, S. A. (1998). *Foundations of social evolution*. Princeton University Press.
- 269 Lynsdale, C. L., Mumby, H. S., Hayward, A. D., Mar, K. U., & Lummaa, V. (2017). Parasite-associated mortality
270 in a long-lived mammal: Variation with host age, sex, and reproduction. *Ecology and Evolution* **7**.24,
271 pp. 10904–10915.
- 272 Osnas, E. E. & Dobson, A. P. (2011). Evolution of virulence in heterogeneous host communities under multiple
273 trade-offs. *Evolution* **66**.2, pp. 391–401. DOI: [10.1111/j.1558-5646.2011.01461.x](https://doi.org/10.1111/j.1558-5646.2011.01461.x).
- 274 Otto, S. P. & Day, T. (2007). *A biologist's guide to mathematical modeling in ecology and evolution*. **13**. Princeton
275 University Press.
- 276 Sukumar, R., Krishnamurthy, V., Wemmer, C., & Rodden, M. (1997). Demography of captive Asian elephants
277 (*Elephas maximus*) in southern India. *Zoo Biology: Published in affiliation with the American Zoo and*
278 *Aquarium Association* **16**.3, pp. 263–272.
- 279 Taylor, P. D. (1990). Allele-frequency change in a class-structured population. *The American Naturalist* **135**,
280 pp. 95–106.